

Electrodeposition of Thin Re–Se Films

E. A. Salakhova

Institute of Inorganic and Physical Chemistry, Academy of Sciences of Azerbaijan,
pr. Dzhavida 29, Baku, 370143 Azerbaijan

e-mail: itpcht@itpcht.ab.az

Received May 18, 2001; in final form, August 13, 2002

Abstract—Re, Se, and Re–Se electrodeposition from alkaline electrolytes was studied. The effects of process variables were examined, and the nature of polarization in the course of rhenium and selenium deposition from alkaline electrolytes was assessed. Re–Se electrodeposition was investigated by the potentiodynamic polarization technique. The codeposition process was shown to be attended by depolarization, which is due to the energy release upon the formation of the alloy.

INTRODUCTION

Rhenium–selenium alloys possess semiconducting properties and are employed as photosensitive elements for the visible range. In most semiconductor devices, rhenium alloys are used in thin-film form [1–3].

In this paper, we report our efforts to prepare thin Re–Se films by electrochemical means. Electrodeposition offers the advantages of simple equipment, relative ease, and low cost and, in some cases, allows one to produce films of controlled composition by adjusting the electrolyte composition and electrolysis conditions.

Earlier [4, 5], Re–Se alloys were prepared using electrolytes consisting of NH_4ReO_4 (10–50 g/l), SeO_2 (10–50 g/l), and H_2SO_4 (200 g/l).

At the same time, it is of interest to use electrolytes containing rhenium and selenium compounds as major constituents in order to produce alloys close in properties to those employed in modern technology.

Here, we describe electrodeposition from 0.01–0.1 M NH_4ReO_4 + 0.01–0.1 M SeO_2 + NaOH alkaline electrolytes.

We prepared Re, Se, and Re–Se films. Particular attention was paid to electrodeposition of thin Re–Se films from alkaline electrolytes. The process was followed by the potentiodynamic polarization technique.

EXPERIMENTAL

Potentiodynamic polarization curves were recorded using a P-5827 potentiostat and PDP4-002 chart recorder. Pt wire and a 0.15-cm² Pt platelet were utilized as the anode and cathode, respectively. All potentials were measured with respect to an Ag/AgCl reference. The electrolyte temperature was maintained constant using a thermostat. The cathode deposit was analyzed for Re and Se. To this end, the deposit was dissolved in concentrated HNO_3 (10 ml) during heating. After long-term boiling on a water bath, 5 N H_3PO_4 was

added to the solution, which was then diluted to 50 ml in a volumetric flask. Next, rhenium was separated from selenium by selective extraction with isoamyl alcohol. Rhenium and selenium were determined by photometric analysis (FEK-56M instrument) of rhodanide and thiourea complexes, respectively [6]. The Re–Se films were characterized by x-ray diffraction (XRD) using a 57.3-mm Debye–Scherrer camera (CuK_α radiation, URS-55 x-ray generator).

RESULTS AND DISCUSSION

We studied the effects of electrolyte composition, current density, and temperature on the electrolysis process.

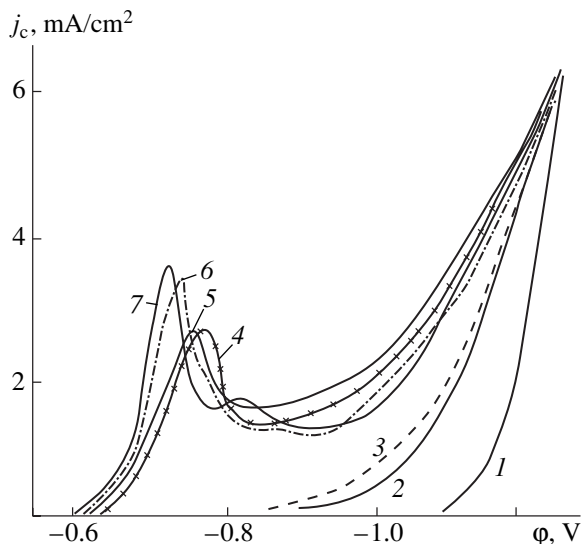


Fig. 1. Polarization curves for (1) a blank solution and (2, 3) Re, (4, 5) Se, and (6, 7) Re–Se electrodeposition at 75°C. Electrolytes: (1) NaOH, (2) NaOH + 0.05 M NH_4ReO_4 , (3) NaOH + 0.08 M NH_4ReO_4 , (4) NaOH + 0.05 M SeO_2 , (5) NaOH + 0.08 M SeO_2 , (6) NaOH + 0.05 M NH_4ReO_4 + 0.05 M SeO_2 , (7) NaOH + 0.08 M NH_4ReO_4 + 0.08 M SeO_2 .

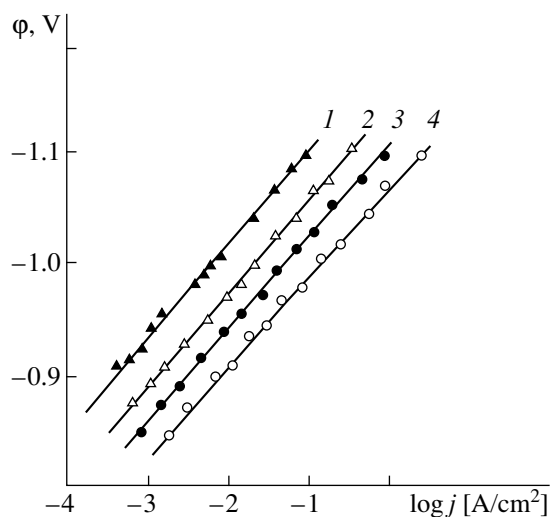


Fig. 2. Polarization plots for solutions containing 1 M NaOH and (1) 0.02, (2) 0.05, (3) 0.06, and (4) 0.09 M NH_4ReO_4 ; $t = 75^\circ\text{C}$.

Figure 1 shows the polarization curves of a blank solution (curve 1) and Re (curves 2, 3), Se (curves 4, 5), and Re–Se (curves 6, 7) electrodeposition. The NaOH concentration and temperature (75°C) were maintained constant. It can be seen in Fig. 1 that increasing the rhenium concentration in the electrolyte increases the deposition rate and shifts the cathode potential to positive values.

At higher rhenium concentrations in the electrolyte, we obtain lustrous, gray, uniform coatings up to $10\ \mu\text{m}$ thick on the cathode surface. At low rhenium concentrations and a current density of $1\ \text{mA}/\text{cm}^2\ \mu\text{m}$, electrodeposition yields lustrous, gray, uniform coatings $\leq 2\ \mu\text{m}$ in thickness.

Rhenium deposition is accompanied by hydrogen release, and hydrogen actively adsorbs on the electrode surface. The rate of hydrogen release depends on the electrolyte composition and current density. The rhenium deposition and hydrogen adsorption on the cathode begin at $-1.0\ \text{V}$. Increasing the magnitude of the potential increases the rate of hydrogen release much

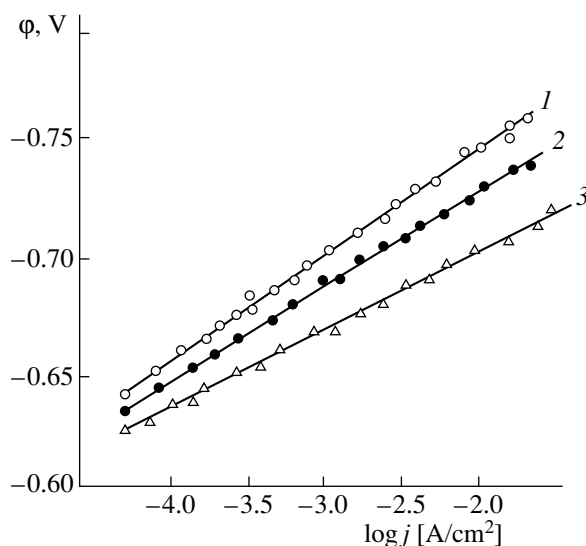


Fig. 3. Polarization plots for solutions containing 1 M NaOH and (1) 0.03, (2) 0.05, and (3) 0.08 M SeO_2 ; $t = 75^\circ\text{C}$.

more rapidly than the rate of rhenium deposition. Under such conditions, the current efficiency in terms of rhenium is 4%. The low current efficiency is due to the low overpotential of hydrogen on rhenium and platinum. Owing to the appreciable hydrogen sorption by rhenium during electrodeposition, rhenium acts as a hydrogen electrolyte, and the potential ($-1.0\ \text{V}$) is determined by the hydrogen saturation of the metal [3].

The current efficiency versus current density data for rhenium electrodeposition are summarized in Table 1. Figure 2 demonstrates that, with increasing rhenium concentration, the cathodic polarization plot shifts to higher potentials, with no change in slope ($\partial\phi_c/\partial\log j_c = 0.1\ \text{V}$).

To gain detailed insight into the mechanism of selenium cathodic deposition in alkaline solutions, we examined the effect of selenium concentration in the electrolyte on cathodic polarization. As seen in Fig. 3, the semilog plot of cathodic polarization shifts to higher potentials with increasing Se concentration in the electrolyte, which points to an increase in the rate of

Table 1. Current efficiency vs. current density data for rhenium electrodeposition from a $0.05\ \text{M}\ \text{NH}_4\text{ReO}_4 + \text{NaOH}$ solution at $t = 75^\circ\text{C}$

$j, \text{mA}/\text{cm}^2$		Current efficiency, %		External appearance of the coating
total	Re deposition	rhenium	hydrogen	
2	0.08	4.0	96	Light gray, lustrous, uniform
5	0.17	3.5	96.5	Light gray, lustrous, smooth
10	0.32	3.2	96.8	Dark gray, dull, smooth
15	0.33	2.2	97.8	Dark gray, lustrous, nonuniform

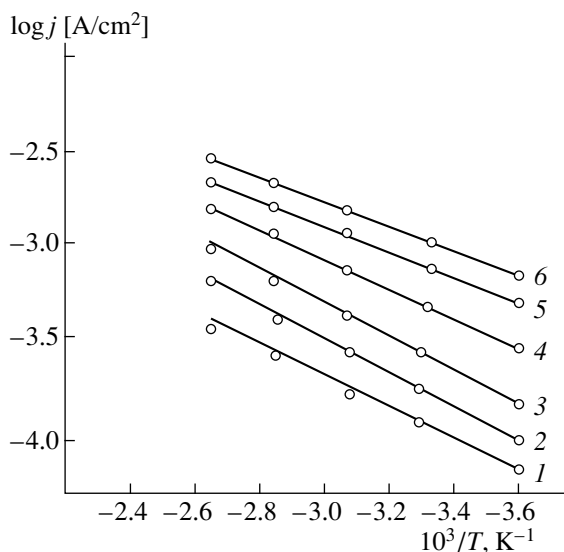


Fig. 4. Temperature dependences of current density at Pt electrode potentials of (1) -0.65 , (2) -0.68 , (3) -0.70 , (4) -0.72 , (5) -0.75 , and (6) -0.80 V.

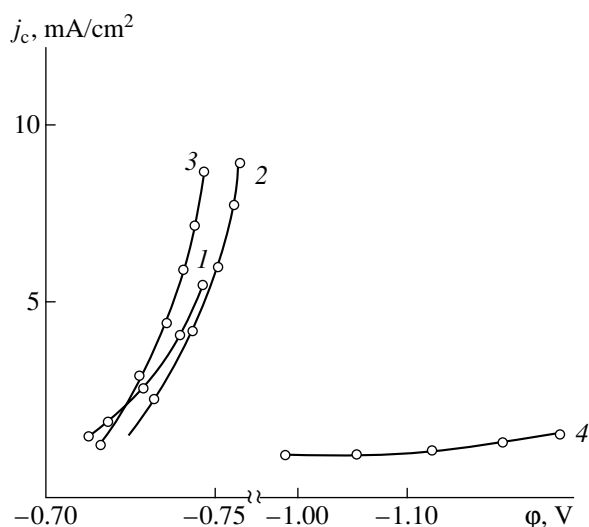


Fig. 6. Partial polarization curves for rhenium and selenium deposition from alkaline electrolytes at 75°C : (1) rhenium in the alloy, (2) elemental selenium, (3) selenium in the alloy, (4) elemental rhenium.

the cathodic process. The slope of the plot is $\partial\phi_c/\partial \log j_c = 0.056\text{--}0.07$ V. These data suggest that, at low current densities, selenium deposition is accompanied by chemical polarization.

The polarization curves of selenium electroreduction from alkaline electrolytes (Fig. 1, curves 4, 5) display a prominent peak at -0.8 V. The polarization curves of Se^{4+} reduction on the platinum cathode in alkaline media consist of three distinct portions, which correspond to the reduction of Se^{4+} to elemental sele-

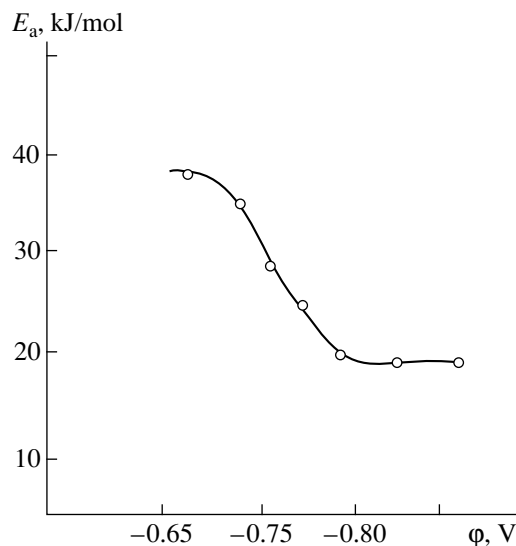


Fig. 5. Apparent activation energy as a function of potential.

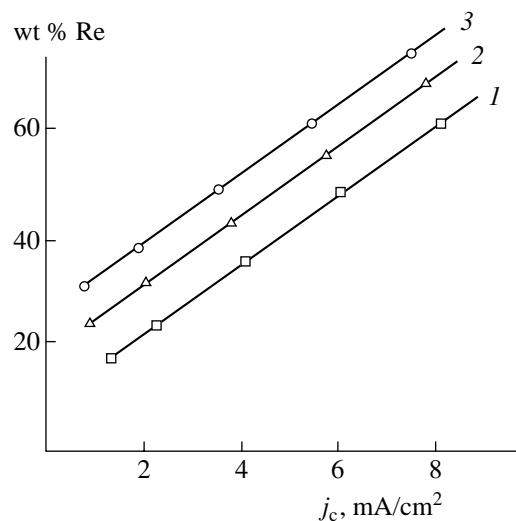


Fig. 7. Rhenium content of the Re–Se alloy as a function of current density at 75°C . Electrolytes: (1) 0.01 M NH_4ReO_4 + 0.09 M SeO_2 + 1 M NaOH, (2) 0.03 M NH_4ReO_4 + 0.07 M SeO_2 + 1 M NaOH, (3) 0.05 M NH_4ReO_4 + 0.05 M SeO_2 + 1 M NaOH.

nium, the formation of Se^{2-} , and hydrogen release:



The formation of Se^{2-} was also reported by Baeshov *et al.* [7], who showed that, with increasing NaOH concentration, the wave in polarization curves disappears.

To identify the rate-limiting step of the cathodic process and the nature of cathodic polarization upon the reduction of SeO_3^{2-} in alkaline electrolytes, we exam-

Table 2. Composition and quality of Re–Se coatings as functions of current density in a 1 M NaOH solution at $t = 75^\circ\text{C}$

Electrolyte, mol/l		j , mA/cm ² (deposition)	Alloy composition, wt %		Light gray, nonuniform
NH ₄ ReO ₄	SeO ₂		Re	Se	
0.05	0.05	2	38.2	61.8	Dark gray, uniform, smooth
0.05	0.05	4	48.4	51.6	Black, lustrous, smooth
0.05	0.05	5	54.0	46.0	Dull black, smooth
0.05	0.05	7	72.1	27.9	External appearance of the coating

ined the temperature effect on the rate of the electrode process at a constant cathode potential. The results are displayed in Fig. 4. From the slope of the lines thus obtained, we evaluated the apparent activation energy of the electrode process (Fig. 5). At potentials from -0.65 to -0.725 V, the apparent activation energy attains 30–35 kJ/mol. With increasing cathodic polarization, the apparent activation energy drops to 20 kJ/mol at -0.8 V and then varies little.

Thus, at cathodic polarizations above -0.785 V, selenium electrodeposition from alkaline electrolytes is accompanied mainly by chemical polarization.

Since selenium deposition on the cathode is attended by the release of a substantial amount of hydrogen, we obtained partial polarization curves in order to gain detailed insight into the electrode processes involved.

Figure 6 shows the partial polarization curves for Re, Se, and Re–Se deposition. From the curves of Re deposition in elemental form and in the Re–Se alloy, it follows that depolarization in the latter case is 350 mV (Fig. 6). For selenium in the alloy, depolarization is 20–30 mV.

As seen in Fig. 1, the curves for Re–Se deposition (curves 6, 7) lie at higher potentials than those for Re and

Se. During the electrolysis of mixtures of alkaline Se and Re solutions, the rate of ReO_4^- and SeO_3^{2-} reduction is higher. This seems to be due to the depolarization effect, associated mainly with the formation of the alloy. Consequently, codeposition of rhenium and selenium must lead to the formation of a compound or solid solution.

Our results demonstrate that, as the current density rises from 2 to 8 mA/cm², the rhenium content of the alloy increases from 20 to 80 wt % (Fig. 7) and the quality of the coating improves (Table 2).

At a cathode current density of 4 mA/cm², using an electrolyte of composition 0.05 M NH₄ReO₄ + 0.05 M SeO₂ + 1 M NaOH, we obtained lustrous ReSe₂ (54 wt % Re) coatings. The formation of ReSe₂ was confirmed by XRD. This compound crystallizes in the triclinic system with lattice parameters $a = 6.7275$ Å, $b = 6.6065$ Å, and $c = 6.7196$ Å. The XRD intensities and d spacings for ReSe₂ are listed in Table 3.

CONCLUSION

Codeposition of rhenium and selenium was shown to be attended by depolarization, which is due to the energy release upon the formation of the alloy.

REFERENCES

1. Savitskii, E.M., Gylkina, M.A., and Levin, A.M., *Splavy reniya v elektrotekhnike* (Rhenium Alloys in Electrical Engineering), Moscow: Energiya, 1980.
2. Savitskii, E.M. and Gylkina, M.A., *Splavy reniya* (Rhenium Alloys), Moscow: Nauka, 1965, p. 175.
3. Sominskaya, M.Z., *Renii* (Rhenium), Moscow: Akad. Nauk SSSR, 1961, p. 209.
4. Salakhova, E.A., Mamedov, M.N., and Novruzova, R.S., Azerb. Inventor's Certificate no. 1240, 1997.
5. Salakhova, E.A., Coreduction of Rhenium and Selenium in Sulfuric Acid Solutions, *Azerb. Khim. Zh.*, 1999, no. 3, pp. 9–12.
6. Borisova, L.V. and Ermakov, A.M., *Analiticheskaya khimiya reniya* (Analytical Chemistry of Rhenium), Moscow: Nauka, 1974.
7. Baeshov, A., Zhurinov, M.Zh., and Zhdanov, S.I., *Elektrokhimiya selena, tellura i poloniya* (Electrochemistry of Selenium, Tellurium, and Polonium), Almaty: Nauka, 1989, p. 53.

Table 3. XRD data for ReSe₂ obtained in an alkaline electrolyte of composition 0.05 M NH₄ReO₄ + 0.05 M SeO₂ + NaOH (at $j_c = 5$ mA/cm² and $t = 75^\circ\text{C}$)

d , Å	I/I_0	hkl	d , Å	I/I_0	hkl
6.380	90	100	2.205	40	121
5.781	40	001	2.183	40	023
4.720	40	101	2.163	40	131
3.240	20	011	2.143	20	012
2.867	60	120	2.130	20	301, 300
2.840	60	102	2.100	40	021
2.696	20	211	2.075	20	031
2.512	90	220	2.043	40	212
2.480	40	–	2.015	20	320
2.469	100	122	1.947	60	103
2.370	40	202	1.880	40	213
2.272	40	127			
2.214	20	112			